



RESEARCH ARTICLE

# Conversion of sugarcane bagasse into cellulose, carboxymethyl cellulose and polymer membrane electrolyte and their characterization

P Vijayakumary<sup>1</sup>, Manisha Reddy B<sup>1</sup>, Meenakshi P<sup>1</sup>, Parimala Devi R<sup>1\*</sup>, Subramanian P<sup>1</sup>, Sriramajayam S<sup>2</sup>, Gitanjali Jothiprakash<sup>1,3\*</sup> & Desikan Ramesh<sup>1</sup>

<sup>1</sup>Department of Renewable Energy Engineering, Agricultural Engineering College and Research Institute, Tamil Nadu Agricultural University, Coimbatore 641 003, Tamil Nadu, India

<sup>2</sup>Department of Agricultural Engineering, V.O. Chidambaranar Agricultural College and Research Institute, Tamil Nadu Agricultural University, Killikulam 628 252, Tamil Nadu, India

<sup>3</sup>Centre for Post Harvest Technology, Agricultural Engineering College and Research Institute, Tamil Nadu Agricultural University, Coimbatore 641 003, Tamil Nadu, India

\*Email: [rimaraj164@gmail.com](mailto:rimaraj164@gmail.com); [jogitanjali@gmail.com](mailto:jogitanjali@gmail.com)



## ARTICLE HISTORY

Received: 16 October 2024

Accepted: 07 November 2024

Available online

Version 1.0 : 31 December 2024



## Additional information

**Peer review:** Publisher thanks Sectional Editor and the other anonymous reviewers for their contribution to the peer review of this work.

**Reprints & permissions information** is available at [https://horizonpublishing.com/journals/index.php/PST/open\\_access\\_policy](https://horizonpublishing.com/journals/index.php/PST/open_access_policy)

**Publisher's Note:** Horizon e-Publishing Group remains neutral with regard to jurisdictional claims in published maps and institutional affiliations.

**Indexing:** Plant Science Today, published by Horizon e-Publishing Group, is covered by Scopus, Web of Science, BIOSIS Previews, Clarivate Analytics, NAAS, UGC Care, etc See [https://horizonpublishing.com/journals/index.php/PST/indexing\\_abstracting](https://horizonpublishing.com/journals/index.php/PST/indexing_abstracting)

**Copyright:** © The Author(s). This is an open-access article distributed under the terms of the Creative Commons Attribution License, which permits unrestricted use, distribution and reproduction in any medium, provided the original author and source are credited (<https://creativecommons.org/licenses/by/4.0/>)

## CITE THIS ARTICLE

Vijayakumary P, Manisha RB, Meenakshi P, Parimala DR, Subramanian P, Sriramajayam S, Jothiprakash G, Ramesh D. Conversion of Sugarcane bagasse into cellulose, carboxymethyl cellulose and polymer membrane electrolyte and their characterization. Plant Science Today.2024;11 (sp4):01-12. <https://doi.org/10.14719/pst.5874>

## Abstract

Petroleum-derived products have long been used as raw materials for synthesizing polymers. The diminished petroleum reserves and growing environmental consciousness have prompted a shift toward sustainable alternatives. Biodegradable organic materials derived from agricultural biomass, offer a promising pathway to produce eco-efficient polymers. Cellulose transformation into carboxymethyl cellulose (CMC) is a focal point, as CMC's water solubility and polymeric characteristics facilitate diverse applications, particularly in energy storage systems. This research aims to study the variations in chemical treatments on biomass, focusing on sugarcane bagasse as a case study. Chemical and steam explosion pretreatments were applied to the bagasse, leading to enhanced cellulose recovery, with cellulose content increasing from 52.7% to 65.4% and overall yield improving from 35.3% to 49.1%. SEM and FT-IR analyses revealed significant structural changes. In contrast, XRD analysis indicated a rise in the crystallinity index from 34.8% in untreated bagasse to 70.5% in treated samples, with a reduction in crystallite size. The synthesis of CMC demonstrated a peak degree of substitution (DS) of 0.82 using 25% NaOH, resulting in CMC with improved solubility and flexibility. CMC films prepared with different binding agents, such as glycerol, demonstrated optimal flexibility, conductivity and mechanical strength, making them suitable for polymer electrolyte applications. Analysis of CMC polymer films highlighted glycerol (15 wt%) as the most effective binding agent, enhancing the film's fold endurance and flexibility. These findings underscore the potential of biomass-derived polymer membranes to replace petroleum-based materials and contribute to sustainable development.

## Keywords

biomass; bagasse; cellulose; energy storage; polymer

## Introduction

Organic materials have a wide range of uses and are primarily sourced from petroleum (1). However, the petroleum supply is being rapidly depleted. Furthermore, new environmental regulations, societal concerns and growing ecological consciousness have created many questions about the petrochemical industry, prompting the search for environmentally friendly products and methods (2). Therefore, biodegradable organic resources, such as polymers, can produce a portfolio of sustainable eco-

efficient products that can compete in markets currently dominated by petroleum-based products. Additionally, biopolymer products derived from biomass and agricultural feedstock can be renewed every year (3). By directly, catalytically, or aggressively converting cellulose, hemicellulose and lignin nearly all petrochemical compounds can be produced from biomass (4). However, because of its insolubility in water, the application of cellulose is limited, but its water-soluble derivatives, particularly carboxymethyl cellulose (CMC), play an essential role in our daily lives (5). The issue is how to modify the structure of cellulose to make it water soluble, so that it can be used in a variety of applications (6). Making polymer electrolytes for energy storage devices will be simpler (7). Recent studies show that biopolymer electrolytes derived from agricultural wastes, such as corn starch, banana peel, rice husk and soybean residue, demonstrate promising ionic conductivities ranging from  $6.5 \times 10^{-4}$  to  $4.3 \times 10^{-3}$  S/cm with applications in energy storage devices like solid-state batteries and supercapacitors (8-11). Additionally, chitosan-based electrolytes reinforced with agro-waste fillers exhibit enhanced mechanical stability, supporting their use in next-generation sustainable batteries (12). The novelty of this research lies in transforming sugarcane bagasse, an agricultural by-product, into cellulose, CMC and a polymer membrane electrolyte, contributing to sustainable material science. It introduces an efficient conversion method to produce water-soluble CMC, enhancing its industrial applications as a biodegradable alternative to petroleum-based products. Additionally, the development of a polymer membrane electrolyte from cellulose derivatives opens new avenues for eco-friendly energy storage solutions. This study combines waste valorization with innovations in sustainable polymers and renewable energy technology.

## Materials and Methods

### Characterization of feedstock

The physiochemical properties of the feedstock are crucial for evaluating its suitability for various applications. These properties are determined through a series of analyses, including proximate, ultimate and compositional analysis (13).

#### Proximate analysis

Proximate analysis is conducted to assess the basic characteristics of the feedstock, focusing on four key parameters. The moisture content, Volatile matter, Ash content and Fixed Carbon content were measured using the standards set by ASTM methods (E 871, E 872, D 482).

#### Ultimate analysis

The ultimate analysis determines the elemental composition of the feedstock. Using the ASTM-D3176-89:2002 standard, this analysis quantifies the percentages of carbon (C), hydrogen (H), oxygen (O), nitrogen (N) and sulfur (S).

#### Compositional analysis

Compositional analysis, following the NREL (National Renewable Energy Laboratory) technique, provides detailed information on the structural components of the feedstock. This analysis includes the estimation of cellulose content (%), hemicellulose content (%) and lignin content (%) (14).

### Chemicals and reagents

Sodium Hydroxide ( $\geq 97\%$ , ACS grade), Sodium Chlorite ( $\geq 80\%$ , Technical grade), N, N-Dimethylformamide (DMF) ( $\geq 99.9\%$ , HPLC grade), Sodium Monochloroacetate ( $\geq 98\%$ , Reagent grade) and Oleic Acid ( $\geq 99\%$ , Reagent grade) were sourced from Sigma-Aldrich. Isopropanol, Methanol, Ethanol, Glacial Acetic Acid ( $\geq 98\%$ , Reagent grade), Glycerol ( $\geq 99.5\%$ , ACS grade) and Oxalic Acid ( $\geq 99\%$ , Analytical grade) were obtained from Merck. Ammonium Nitrate ( $\geq 99\%$ , Analytical grade) was purchased from Fisher Scientific.

### Pretreatment of feedstock for cellulose extraction

This study employed two pretreatment methods to extract the cellulose from the selected biomass feedstock. The chemical pretreatment methods included alkaline and acid pretreatment. Additionally, steam explosion (SE) pretreatment will be applied to the biomass feedstock to extract cellulose (15).

Chemical treatment involves five steps to extract the cellulose from the biomass feedstock. The first step involves the alkali treatment of the fibre which involves the fibres being placed in the different NaOH (1.5, 2, 5 and 7.5%) concentrations. The next step consists of an autoclave process in which NaOH-treated fibres were autoclaved at high pressures (60, 103, 115 and 120 Pa for 1, 1.5, 2 and 2.5 h). The next step involves the bleaching of the fibre. Sodium chlorite is the best bleaching agent, which was used at different concentrations (2, 5, 10 and 15%) and was placed into this solution for 0.5, 1, 1.5 and 2 hours at 40, 50, 70 and 80 °C using laboratory magnetic stirrer. The final step involves the acid treatment of the fibre by (2, 5, 7.5 and 10%) oxalic acid. Bleached fibres will be soaked into these oxalic acid concentrations for (1, 1.5, 2 and 2.5 hours) (16).

Despite the steam explosion, pretreatment of biomass uses steam at high temperatures (160-280 °C) and high pressures (0.7-4.8 MPa) for 5-30 min (17). In this study, steam explosion pretreatment was done at 192, 200 and 205 °C for 5-15 min. under high pressures (13, 15 and 17 bar). To make the steam explosion more efficient catalysts NaOH, water and citric acid have been used to get better yields.

### Synthesis of extracted cellulose, carboxymethylcellulose and polymer electrolyte membrane

The process of synthesis of CMC from extracted cellulose is illustrated in Fig. 1. In a flask, 10 mL NaOH (15, 25 and 35% concentrations) and 30 mL of isopropanol were used to dissolve 3 g of dry cellulose. With the magnetic stirrer, the alkalization of the sample was carried out for 60 min at 30 °C. The carboxymethylation process was carried out by stirring the sample with sodium mono-chloroacetate (3 g) for 3 hours at 50 °C to complete. The above mixture was suspended in the methanol solution and the solution was filtered. The glacial acetic acid was used to neutralize the filtered residue. Following this, the ethanol was used to wash the residue, filtered and dehydrated at room temperature for six hours. Glacial acetic acid was used to neutralize and suspend it in methanol. Afterwards, the residue was filtered again, rinsed with ethanol and dehydrated at room temperature for another six hours. The yield of carboxymethyl cellulose is the ratio of the weight of prepared CMC to the weight of dried cellulose in percentage depending on the dried weight of CMC and cellulose (18). To 40 mL of distilled water, 100 mg of carboxymethyl cellulose was dissolved, to

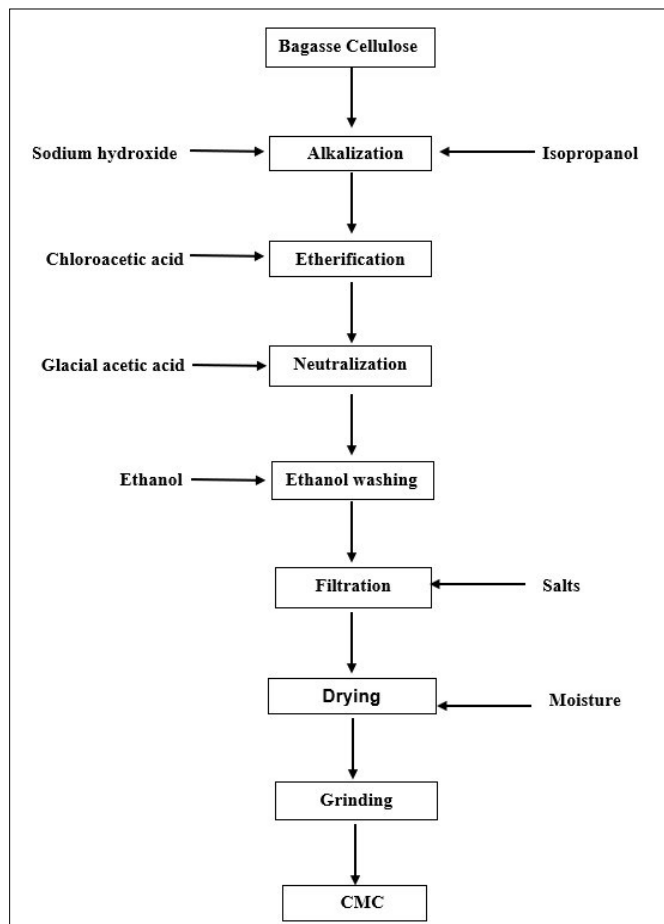


**Fig. 1.** Flow chart of CMC extraction process from bagasse cellulose.

achieve the desired porosity, different binding agents like N, N-dimethylformamide (2.5 mL), oleic acid (20 wt%), ammonium nitrate (25 wt%) and glycerol (15 wt%) were added to the CMC solution was vigorously swirled at 70°C, lead to a transparent solution. After 4 hours of stirring and casting on a glass plate, a thin CMC membrane, roughly 20 mm thick, was formed when the water was evaporated at 80°C. The membrane was subjected to vacuum drying at 80°C for 24 hours. Simultaneously, commercial CMC will be obtained from the laboratory and a polymer electrolyte will be made and compared to the commercial polymer electrolyte (19).

#### **Characteristics of extracted cellulose, carboxymethylcellulose and polymer electrolyte membrane**

Structural analysis (X-ray diffraction) of the materials was performed using Bruker AXS D8 diffractometer at  $\text{CuK}\alpha$   $\lambda = 1.54060 \text{ \AA}$ , operating at 40 kV and 30 mA, with a scan rate of 5° per minute. The Scherrer analysis was used to determine the crystallite size of the samples. The examination of structural and functional groups of all samples was done by using FTIR spectroscopy (Bruker, USA). Using KBr (1:100 w/w), 2 mg of dry materials were compressed into a pellet. Wave numbers between 4000–400  $\text{cm}^{-1}$  measure the transmission level.

The morphology of raw material, extracted CMC and cellulose were examined. The morphological properties of raw fibres, cellulose and CMC. A field emission scanning electron microscope (FE-SEM, S-4800, Japan) running at a 10 kV acceleration voltage was used to create CMC films, with 1000x original magnifications for getting high-resolution images and 10  $\mu\text{A}$  of current following sample coating with a vacuum sputter coater (20). The degree of substitution of carboxymethylcellulose,

which varies from 0 to 3, is the mean number of sodium carboxymethyl groups attached / unit of anhydrous glucose. The titration (back & direct) and precipitation with copper are employed to determine carboxymethyl cellulose DS. To remove byproducts, CMC was thoroughly cleaned with 80%  $\text{CH}_3\text{OH}$  and  $\text{CH}_3\text{OH}$ . Then at 80°C, two grams of it was dissolved in 50 mL of double-distilled  $\text{H}_2\text{O}$  and agitated for 15 min. to ensure complete dissolution and then centrifuged for a minute at 4000 rpm to remove the precipitated solids. 50 mL of pure  $\text{CH}_3\text{COCH}_3$  were then used to re-precipitate the dissolved CMC. After that, the recovered CMC was filtered and dried at 70°C in an oven until its weight remained constant (21). CMC purity (%) is the ratio of the weight of the dried residue to the weight of the specimen utilized (22). 90 mL of distilled water was used to dissolve 2.7 g of CMC that had been weighed in a 100 mL beaker. The viscosity of the 2.7 g CMC dissolved in 90 mL distilled  $\text{H}_2\text{O}$  at 80°C for 10 min. with 960 rpm for 10 seconds in a magnetic stirrer. The spindle (with the protection connected) was placed into the solution as soon as it was finished. At 5-minute intervals, the sample's temperature was changed between 30, 40, 50 and 60 °C while the speed was kept constant at 160 rpm until the test was completed (23).

A Chroma meter (CR-200, Japan) was used to examine the surface color of all samples. As a traditional backdrop colour, a white colour plate ( $L = 97.75$ ;  $a = -0.49$ ;  $b = 1.96$ ) was chosen. Hunter L, a and b (L: brightness, a: greenness-redness and b: blueness-yellowness) values were calculated by taking measurements at random positions on each film sample (24). To evaluate the water solubility, the film was divided into a square (20 × 20 mm). After 2 hours of immersion in distilled water (50 mL), the film specimen was shaken frequently. After filtering, the residue was dried for 24 hours at 105°C (25). A manual fold endurance test was performed on film samples that were about 0.03 mm thick. The logarithm of the number of double folds required to induce failure in a test specimen under laboratory conditions. (26). Using a micrometer model GT-313-A (Gotech Testing Machine Inc., China), the thickness of the CMC films was determined. A universal texturometer (Model 1000 HIK-S, UK) was used to test the CMC films' tensile strength (TS) and percentage elongation at break (EB) ten times each, in compliance with ASTM D882-80a (27) standard procedure with preconditioning for 24 hours and the results were obtained at 27±2 °C. According to Thai industrial regulations for oriented polypropylene film (TIS 949-2533), the relative humidity (RH) should be 65±2 percent. The rectangular CMC films were cut into 15 mm by 140 mm rectangles to serve as test specimens. The specimens were tested to a crosshead speed of 20 mm/min and an initial grip separation of 100 mm. Impedance measurements of the polymer electrolyte films were conducted using a Solartron 1260 impedance/gain phase analyzer at frequencies ranging from 10 Hz to 4 MHz. Each polymer electrolyte film sample was positioned between two 2.0 cm diameter stainless steel electrodes (area = 3.142  $\text{cm}^2$ ). Temperatures between 303 K and 338 K were used to measure the impedance of the samples. The ionic transference number and electrochemical stability of biopolymer electrolyte sheets were evaluated using the ZIVE MP2. The electrochemical stability window of the biopolymer electrolytes (Seol, Korea) was evaluated using the linear sweep voltammetry (LSV) technique on a Wonatech ZIVE MP2 multichannel electrochemical workstation. The LSV was carried out between 0 and 4 V at a scanning rate of 1  $\text{mV s}^{-1}$  using stainless steel electrodes (28).

The prepared polymer electrolyte has been evaluated by constructing a simple energy storage device. Normally for the preparation of any energy storage device, the essential components are the electrodes and the electrolyte. One electrode of aluminium sheet and another electrode of copper sheet were used and the prepared polymer electrolyte membrane (CMC film) served as both the separator and the electrolyte. The prepared polymer electrolyte film will be sandwiched between the two electrodes. Then it was connected to the two terminals of the voltmeter for voltage values (29).

### Statistical analysis

All experiments were conducted in triplicate ( $n = 3$ ) to account for variability and enhance the reliability of the results. Results are presented as the mean values with standard deviations (Mean  $\pm$  SD), providing a measure of the variability within the dataset.

## Results and Discussion

### Characterization of sugarcane bagasse

The composition of the selected sample is presented in Table 1. Bagasse has the highest oxygen percentage (46.16%), low volatile matter (69.92%) and low bulk density (119.09 kg/m<sup>3</sup>).

### Synthesis of cellulose from pretreatment methods

The most common acid used in chemical treatments is sulfuric acid (H<sub>2</sub>SO<sub>4</sub>). It is widely used, although it has several disadvantages, including the production of inhibitory compounds and reaction vessel corrosion (30). Unlike acid treatment, alkali pretreatment is typically conducted at room temperature and atm. pressure. Common alkaline agents are ammonium, calcium, sodium and potassium hydroxides. The most effective of these hydroxyl derivatives was determined to be sodium hydroxide (31,32). By decomposing the side chains of esters and glycosides, alkali reagents produce lignin structural change, cellulose swelling, cellulose decrystallization and

**Table 1.** Physicochemical properties of sugarcane bagasse

Properties	Value
Moisture content (%)	9.30 $\pm$ 0.051
Volatile matter (%)	69.92 $\pm$ 0.128
Ash content (%)	3.10 $\pm$ 0.042
Fixed carbon (%)	14.20 $\pm$ 0.535
Carbon (%)	44.49 $\pm$ 0.303
Hydrogen (%)	5.92 $\pm$ 0.112
Nitrogen (%)	0.80 $\pm$ 0.023
Sulphur (%)	0.06 $\pm$ 0.001
Oxygen (%)	46.16 $\pm$ 0.136
Cellulose (%)	52.70 $\pm$ 0.433
Hemicellulose (%)	25.13 $\pm$ 0.302
Lignin (%)	20.10 $\pm$ 0.185
Bulk density (kg/m <sup>3</sup> )	119.09 $\pm$ 1.071

**Table 2.** Comparison of compositional analysis of optimized pretreatment condition

Composition	Sample	Value
Cellulose (%)	Raw biomass	52.70 $\pm$ 0.265
	Chemical treated	55.70 $\pm$ 0.435
	Steam treated	65.40 $\pm$ 0.519
Hemicellulose (%)	Raw biomass	25.13 $\pm$ 0.682
	Chemical treated	11.00 $\pm$ 0.871
	Steam treated	7.60 $\pm$ 0.129
Lignin (%)	Raw biomass	20.10 $\pm$ 0.245
	Chemical treated	15.30 $\pm$ 0.072
	Steam treated	1.10 $\pm$ 0.020
Cellulose yield (%)	Chemical treated	35.30 $\pm$ 0.961
	Steam treated	49.10 $\pm$ 1.292

hemicellulose solvation (33). A comparison of different pretreatment methods was conducted by analyzing the composition of cellulose under optimized conditions (Table 2).

NaOH treatment removes a fraction of the lignin, hemicellulose and oil covering on the outside. When external cellulose microfibrils depolymerize and defibrillate, short-length crystalline fibers are produced. The material will expand into the autoclave equipment due to rapid depressurization. The alkali-treated fibres broke when the pressure dropped quickly because the steam at high pressure had damaged their structure. The bleaching process reduces the amount of lignin and other binders in the raw and bleached fibre. After that, the fibers are hydrolyzed with oxalic acid, which combines with the fiber's sodium derivative to produce pure cellulose (34). The most popular chemical pretreatment for enhancing the enzymatic hydrolysis of different biomass types is the alkali method. Because of its remarkable delignification capability, critical for high biomass digestibility, sodium hydroxide (NaOH) has attracted the most attention (35). Fig. 2 depicts the cellulose fibres obtained from bagasse and cellulose after grinding.

Before being injected into the SE reactor, the proper catalyst is impregnated into the lignocellulosic biomass in an acid-catalyzed steam explosion. Enhanced hydrolysis rate, total hemicellulose removal and the ability to operate at lower pretreatment temperatures and residence times, are some benefits of acid catalysts (36). Acid catalysts have various advantages, including improved hydrolysis rate, full hemicellulose removal and the ability to operate at lower pretreatment temperatures and residence times (37). Particle size, temperature, moisture content and residence time are the main determinants of SE pretreatment. Heat transmission and steam consumption are significantly influenced by the feedstock's particle size and moisture content (38).

Small biomass particles allow for better and faster heat transfer inside the reactor, while too large particles might cause surface overcooking, the formation of breakdown products and incomplete hydrolysis of the interior biomass (25). If the biomass contains too much moisture, water will seep into the pores, causing the heating process to shift to operating temperature and initiate autohydrolysis. Temperature and residence time affect SE operation. It is tough to choose between working at high temperatures for short periods versus low temperatures for longer periods and it should depend on the raw material and pretreatment methods. Among the two pretreatment methods, good recovery of cellulose extraction has been observed in the sugarcane bagasse through the steam explosion pretreatment method. The cellulose and yield percentage increased from 52.7% to 65.4% and 35.30% to 49.10% respectively.



**Fig. 2.** Cellulose fibres obtained from bagasse and cellulose after grinding.




Table 3 displays the % yield of CMC produced using various NaOH concentrations. Because cellulose reacts with monochloroacetic acid (MCA) in an alkaline environment, replacing the hydroxyl group of the cellulose molecule with a carboxymethyl group and increasing its weight, the percentage yield of CMC rose as the concentration of NaOH increased. However, at too high a concentration of NaOH, the cellulose may be depolymerized, which affects the DS decline (39).

### Characterization of extracted cellulose and carboxymethylcellulose

#### XRD analysis

Fig. 3 depicts the XRD patterns of sugarcane bagasse at different stages (Raw biomass, chemically treated fibres & steam exploded fibres) and CMC with different NaOH concentrations. Major diffraction intensities at  $22.6^\circ$  and  $18.5^\circ$  are obtained in all samples, confirming the samples are cellulose type. Table 4 gives the XRD analysis and the crystallite size of the samples at various stages. The results show that the crystallinity index increased

**Table 3.** Synthesised CMC yield, purity and solubility at varying NaOH concentrations

CMC synthesised at different concentrations of NaOH	CMC Yield, %	Purity of CMC, %	Solubility of CMC (%)
	15%	98.30	36.27
	25%	120.3	61.50
	35%	101.3	50.53

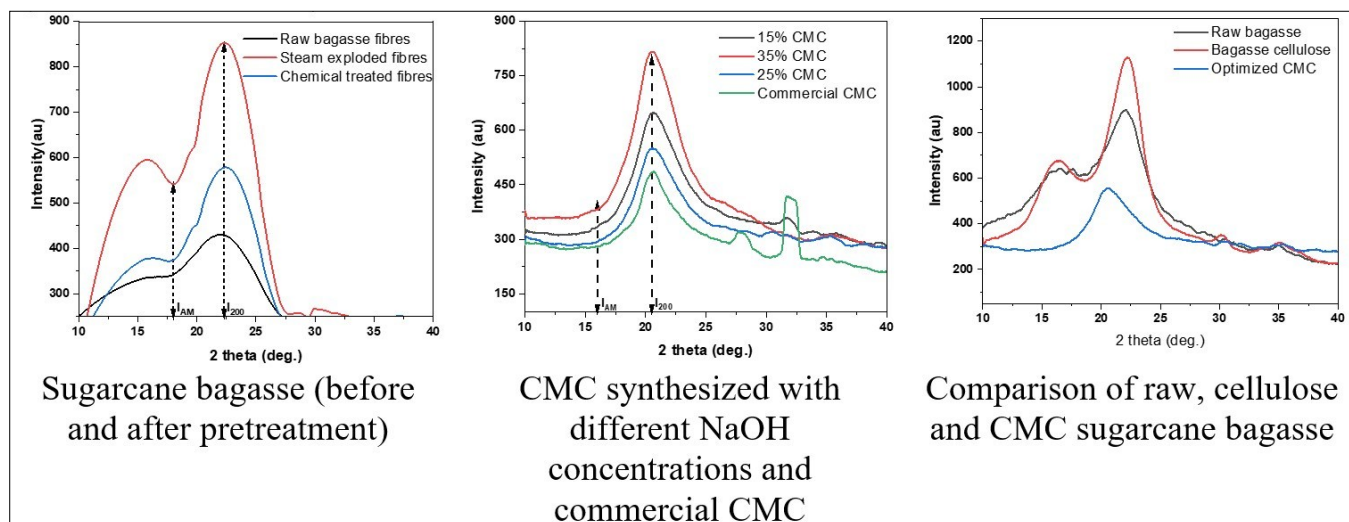


**Fig. 3.** X-ray diffractograms.

**Table 4.** XRD analysis of extracted cellulose and CMC

Crystallinity index (CrI) (%) of extracted cellulose	Raw biomass	34.8
	Chemical treated	64.40
	Steam treated	70.50
Crystallite size (nm) of extracted cellulose	Raw biomass	2.51
	Chemical treated	1.32
	Steam treated	1.03
Crystallinity index (CrI) (%) of extracted CMC	15% NaOH- CMC	45.67
	25% NaOH- CMC	32.13
	35% NaOH- CMC	50.81
Crystallinity index (CrI) (%) of commercial CMC	Standard	30.54

from 34.8% to 70.50%. The raw bagasse crystallite size was 2.51 nm, while the chemically treated and steam-exploded cellulose samples had crystallite sizes of 1.32 and 1.03 nm, respectively. Due to the exposure of the fibres to high pressures, temperatures and reaction periods followed by the bleaching procedure, the crystallite size of steam-exploded cellulose samples was reduced compared to chemically treated cellulose samples (40).

Crystallinity and hydrogen bond strength affect the microstructure of CMC materials. When compared to cellulose derived from sugarcane bagasse, all CMC samples exhibited minimum intensity peak values (au). The decrease in cellulose's crystallinity index may be due to molecule restructuring or breaking in reaction to the alkalization of the NaOH solution and water in the crystallites. The larger aperture among cellulose polymer molecules was also induced by the easy substitution of monochloroacetic acid molecules into the hydroxyl group of cellulose macromolecules without treating it with an alkali solution (41). When various NaOH concentrations were used to alkalize, the crystallinity index decreased. 25% NaOH- CMC has given the least crystallinity index of 32.13%.

#### FTIR Analysis

Fig. 4 shows an FTIR study of materials before and after treatments. The functional groups common to both cellulose and each CMC variant include the hydroxyl group (-OH stretching) observed between  $3200-3600\text{ cm}^{-1}$ , the C-H stretching vibration at  $3000\text{ cm}^{-1}$ , the carbonyl group (C=O stretching) at  $1600\text{ cm}^{-1}$ , the hydrocarbon groups (-CH<sub>2</sub> scissoring) at  $1450\text{ cm}^{-1}$  and the ether groups (-O- stretching) within the range of  $1000-1200\text{ cm}^{-1}$ . The predominant peaks in all spectra were attributed to the stretching vibrations of the -OH and -CH groups, located

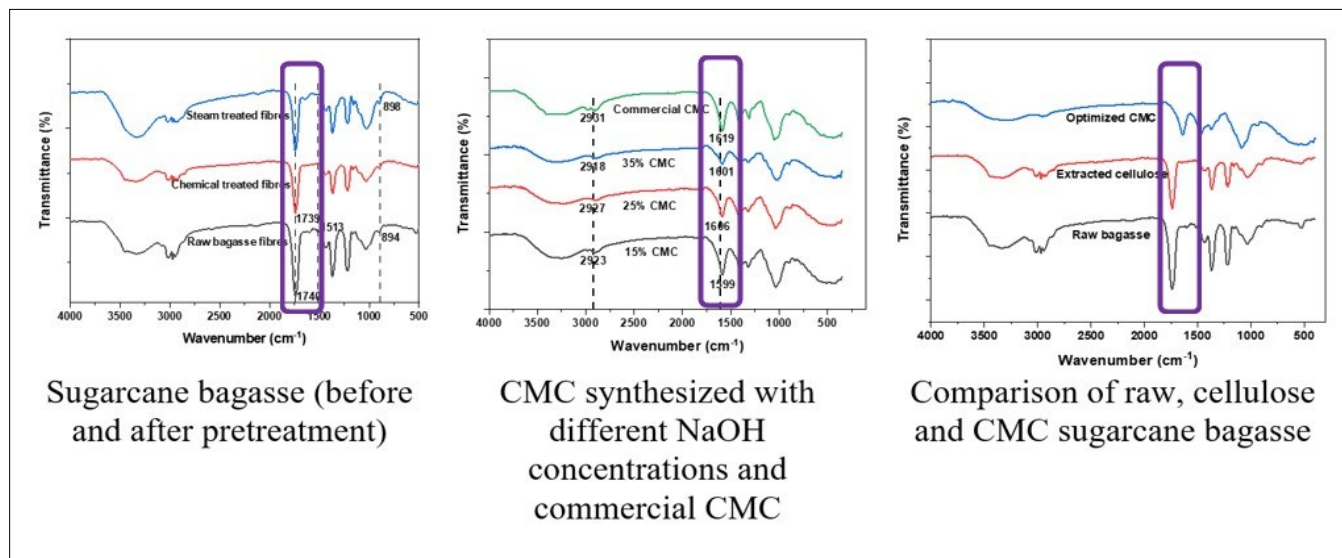


**Fig. 4.** FTIR spectra of bagasse (raw & pretreated), CMC (synthesized at different NaOH conc. & comparison of raw bagasse, cellulose & CMC).

between 3600 and 2800 cm<sup>-1</sup>. In the spectra of the raw fiber, ester linkages were formed by the carboxylic groups of lignin's ferulic and p-coumaric acids, as well as the acetyl and uronic ester groups from hemicelluloses.

The peak remained noticeably weaker and moved to a lower wavenumber in the spectra of cellulose samples that had undergone chemical treatment. This was attributable to the autoclave stage's partial hydrolysis of hemicellulose and pectin. Steam-treated cellulose samples have stronger peaks in their spectra. Bleaching with hydrogen peroxide changed cellulose to oxycellulose, which resulted in the replacement of some hydroxyl groups with ketone groups. Conversely, ester groups may be produced when cellulose and acetic acid react. Furthermore, the addition of additional steric hindrance ester groups to the cellulose surface made filtering easier in the future. This peak in the raw fiber spectra became sharper as the relative lignin concentration increased (5).

The absence of a peak at 1032 cm<sup>-1</sup> in the spectra of the steam-treated cellulose samples indicates that the bleaching process effectively removed lignin. Cellulose's crystalline band aligned with the 527 cm<sup>-1</sup> peak. As further treatments were applied, the peak in the spectra became more pronounced. The pretreatment methods for sugarcane bagasse effectively removed hemicellulose and lignin; for example, the hemicellulose spectra decreased from 1369 to 1361 cm<sup>-1</sup> and lignin spectra decreased from 1359 to 1338 cm<sup>-1</sup>.

The carboxymethylation of bagasse cellulose was confirmed through FTIR analysis after the production of carboxymethyl cellulose (CMC) using varying concentrations of NaOH. The results showed a significant increase in the presence of carbonyl (C=O), ether (-O-) and methyl (-CH<sub>2</sub>) groups in the CMC samples. Notably, peaks at 1606 cm<sup>-1</sup> and 2927 cm<sup>-1</sup> in the CMC samples are associated with the C=O bond, indicating the successful substitution of carboxymethyl groups, as evidenced by the intensity of these peaks. Among the different NaOH concentrations tested, a 25% NaOH solution resulted in the highest degree of carboxyl group substitution in CMC. In contrast, the spectra of steam-treated cellulose samples did not display a peak at 1032 cm<sup>-1</sup>.

### Scanning electron microscopy (SEM) analysis of CMC

Cellulose microfibrils connected by lignin and hemicellulose make up the fiber. Before the cellulose was extracted, there were materials covering the fiber surface, maybe lignin and hemicellulose, which encrusted the cellulose inside. Raw biomass fibres have a high percentage of extractive layers on their surface, which are composed of fibre and pith. The surface of the fiber has a high aspect ratio and is composed of parallel stripes. The initial coarse fibers were significantly larger in diameter and each fiber appeared to be composed of multiple microfibrils. Dense fibre cells with thick walls connect the surface to the pith. The fibres are striped in parallel and have an extractive coating on the outside. The chemically treated defibrillated fibres are obtained after the removal of hemicellulose and other residual extractives (42).

Non-cellulosic substances called lignin and hemicelluloses combine to create a network that connects the fiber bundles to create a structure resembling a composite. The alkali treatment reduces the network's integrity by removing hemicelluloses, which allows certain lignin components to separate and leach out. Following a de-lignification procedure using acidified sodium chlorite, further extractives will be employed to confirm that lignin has been removed. When hemicellulose is hydrolyzed by acids, it produces a liquid phase with a higher xylose content and a lower lignin content. The elimination of non-cellulosic components leads to a slight reduction in the diameter of the fibrils. Steam explosion partially hydrolyses hemicellulose and pectin, loosening the cell wall structure. The raw fibers exhibited bundles resembling a solid web, a result of H<sub>2</sub>O<sub>2</sub> bleaching that eliminated lignin and reduced the number of binding components. At higher magnification, a close examination of the microfibril surface reveals it is nearly free of pits, although boundary fringes can be observed in various areas. Scanning electron microscopy (SEM) images of a single microfibril at 1000x magnification show the formation of numerous terraces, steps and breaks following the cleaning process (Fig. 5.) The diameter of the cellulose extracted from the bagasse has decreased compared to the other cellulose fibres from 1.32 to 1.03. The morphology of CMC powder with varying NaOH concentrations was also assessed using SEM. The samples' microstructure changed as the concentration of NaOH increased. When 15% NaOH was applied to CMC powder, the resultant morphology was small fibres with minimal damage (Fig. 6). As the

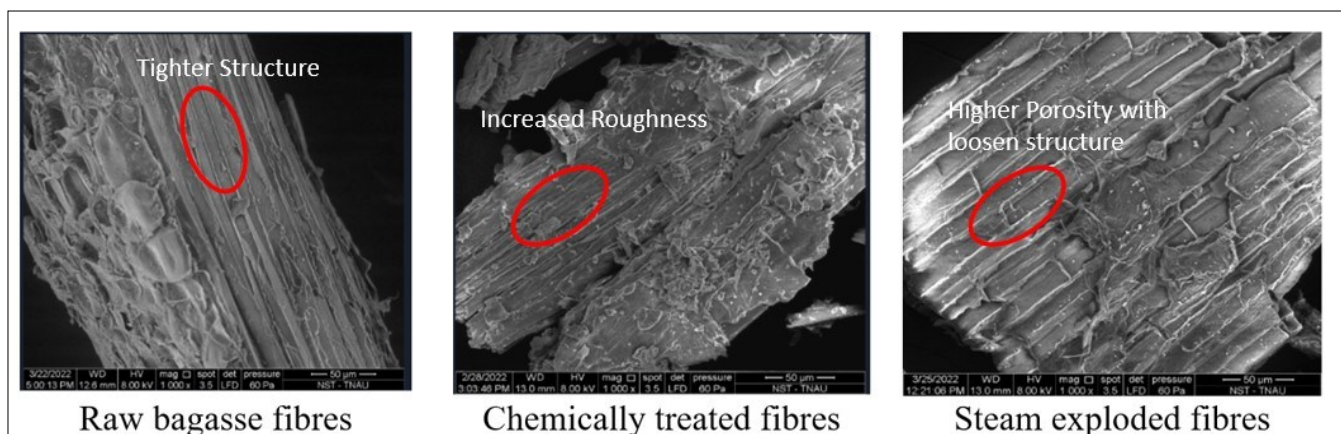


Fig. 5. SEM micrographs of raw and pretreated fibres of bagasse.

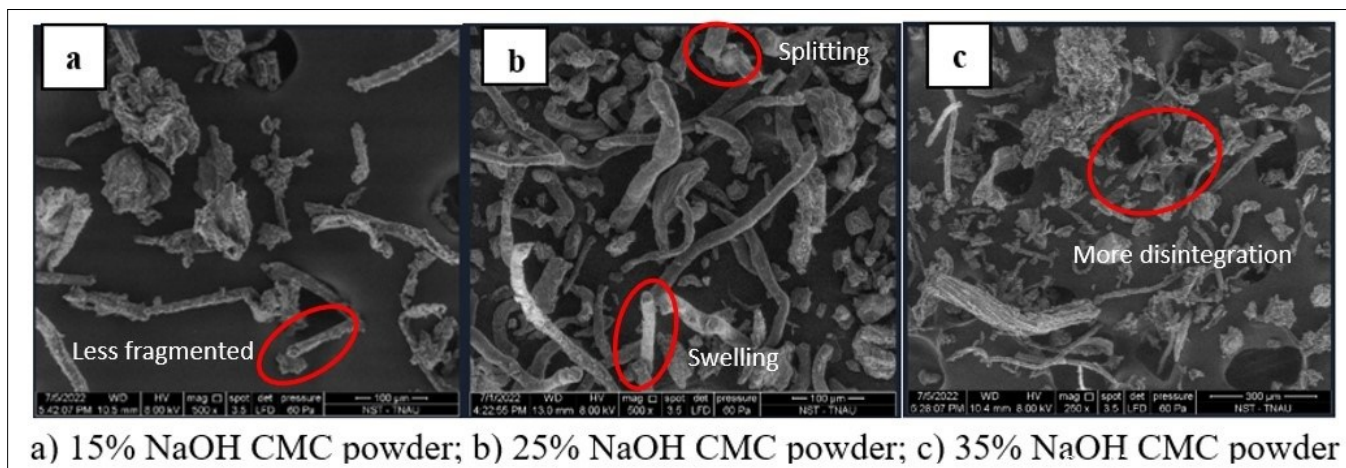


Fig. 6. SEM micrographs of CMC powder.

proportion of NaOH was increased from 15%, 25% and 35% (w/v), the surface homogeneity decreased and 25% NaOH concentration resulted in little fibres with little damage. Exposure to a 35% NaOH concentration caused the surface of the CMC powder to crack and deform, resulting in the degradation of the CMC polymer chain. As the NaOH concentration is increased, the CMC powder's surface develops more cracks and waviness.

The surface was more severely and completely distorted after CMC treatment. This behaviour could therefore indicate that the excessive NaOH content damages the cellulose powder's surface area. This result was comparable to synthetic carboxymethylcellulose produced from bagasse cellulose. The alkaline solution may have weakened the cellulose's structure, lost its crystallinity and changed the chemical structure's stability, making it easier for etherifying agents to reach the molecules for carboxymethylation processes (43). Therefore, this outcome was consistent with DS.

#### Degree of substitution of CMC

The degree of carboxyl group substitution in carboxymethyl cellulose (CMC) can be evaluated using potentiometric titration and infrared (IR) spectroscopy. The values obtained from IR spectra represent relative degrees of substitution ( $DS_{rel}$ ), while

those from potentiometric titration correspond to absolute degrees of substitution ( $DS_{abs}$ ). Table 5 displays the  $DS_{abs}$  and  $DS_{rel}$  for CMC powder synthesized at various NaOH concentrations. At a 25% (w/v) NaOH concentration, the methine (C-H) stretching vibration exhibits an absorbance at  $2927\text{ cm}^{-1}$  and the carboxyl stretching vibration (COO) shows an absorbance at  $1606\text{ cm}^{-1}$ . This is attributed to the ability of monochloroacetic acid (MCA) to easily access the atoms at C2, C3 and C6 of the anhydro-glucopyranose unit, as the crystalline structure of cellulose transitions to an amorphous state. CMC produced the highest yield at this 25% NaOH concentration. The results indicate that CMC output increases with rising  $DS_{abs}$  values. The DS values obtained for CMC range from 0.32 to 0.82, with solubility characteristics dependent on the degree of substitution. Specifically, DS values between 0.0 and 0.4 indicate that CMC is insoluble but swellable, while values above this range indicate complete solubility in water. The highest DS value is associated with CMC synthesized using 25% NaOH. As a result, the cellulose chain and etherifying agent may react more readily to produce the CMC. However, the  $DS_{abs}$  began to decline at higher concentrations of NaOH (>25%), which could be related to the creation of sodium glycolate as a by-product in the synthesis of CMC and the degradation of the cellulose polymer (44).

Table 5. Degree of substitution and absorbance value of synthesised CMC

Type of powder	Obtained results, mL	Average volume of HCl, mL	$DS_{abs}$	$DS_{rel}$	Absorbance at $1606\text{ cm}^{-1}$	Absorbance at $2927\text{ cm}^{-1}$
15% NaOH - CMC	58.3, 57.2, 55.4	56.90	0.43	1.02	0.28100	0.27502
25% NaOH - CMC	42.1, 41.0, 40.6	41.26	0.82	1.32	0.54825	0.41236
35% NaOH - CMC	63.2, 61.8 60.7	61.90	0.32	1.10	0.27613	0.24897

### Viscosity of CMC

Many factors can impact CMC viscosity, including its content, sodium hydroxide concentration and temperature. The viscosity of the produced CMC at 30, 40 and 50 °C is shown in Table 6. The outcome demonstrates that at higher temperatures, viscosity decreased. This is because a higher temperature can both decrease cohesive forces and speed up molecular exchange, which would result in less viscosity. The CMC viscosity evolution followed a similar pattern at the same temperature. In line with earlier DS findings, it rose with NaOH concentrations up to 25% before declining. The DS value seems to be impacted by CMC viscosity. The group that is carboxymethyl is hydrophilic. Therefore, the mechanism achieves more immobilized water depending on the DS (45).

**Table 6.** The viscosity of synthesized CMC at different NaOH concentrations

Sample	Temperature (°C)	Viscosity (cp)
15% NaOH - CMC	30	65.2 ± 0.328
	40	51.9 ± 0.830
	50	42.3 ± 0.547
25% NaOH - CMC	30	81.3 ± 0.846
	40	69.1 ± 0.108
	50	62.6 ± 0.277
35% NaOH - CMC	30	42.7 ± 0.451
	40	39.2 ± 0.222
	50	38.5 ± 0.606

### Preparation of polymer electrolyte membrane

The CMC extracted from the bagasse cellulose has been used for the preparation of various concentrations of CMC films. Four different types of CMC films have been prepared with varied concentrations and with distinct binding agents (Fig. 7). Glycerol, ammonium nitrate, N, N-dimethylformamide (DMF) and oleic acid are the different types of binding agents that have been used. When compared to the other four CMC films, 15 wt% glycerol formulation demonstrated good flexibility and produced a well-formed CMC film. Glycerol is mostly used for energy storage and is generally regarded as safe and non-toxic. A prostereogenic centre is located at position C2 of glycerol, a basic polyol with two primary and secondary hydroxyl groups. Glycerol can undergo a variety of chemical processes, including esterification, selective oxidation, dehydration and hydrogenolysis, to yield a variety of valuable small molecule building blocks with increased chemical complexity for both polymer and small molecule chemical synthesis. Due to all these reasons, glycerol-based polymers are gaining popularity in both theoretical studies and practical applications. Next to the glycerol film, N, N-dimethylformamide (2.5mL) film had some flexibility. CMC films with oleic acid 20 wt% and ammonium nitrate 25 wt% have given some brittle nature with low flexibility (46).

**Table 7.** Color values of Bagasse cellulose, synthesized CMC at different NaOH concentrations and CMC films with different binding agents

Sample	L	a	b	ΔE
Bagasse cellulose	42.49 ± 0.268	2.14 ± 0.018	7.31 ± 0.016	3.80 ± 0.018
15%- CMC	50.26 ± 0.441	2.73 ± 0.032	4.51 ± 0.027	9.10 ± 0.030
25%- CMC	53.50 ± 0.525	3.28 ± 0.037	5.40 ± 0.038	11.92 ± 0.367
35%- CMC	49.84 ± 0.691	2.34 ± 0.048	5.96 ± 0.047	19.28 ± 0.048
CMC film- glycerol (15 wt%)	57.21 ± 0.882	-0.29 ± 0.061	3.22 ± 0.053	5.55 ± 0.062
CMC film-Ammonium nitrate (25 wt%)	57.00 ± 0.048	0.05 ± 0.051	3.58 ± 0.063	5.09 ± 0.082
CMC film- N, N-dimethylformamide (2.5mL)	54.38 ± 0.184	1.41 ± 0.082	4.81 ± 0.071	2.88 ± 0.082
CMC film- Oleic acid (20 wt%)	52.43 ± 0.311	0.13 ± 0.090	4.51 ± 0.079	3.44 ± 0.092

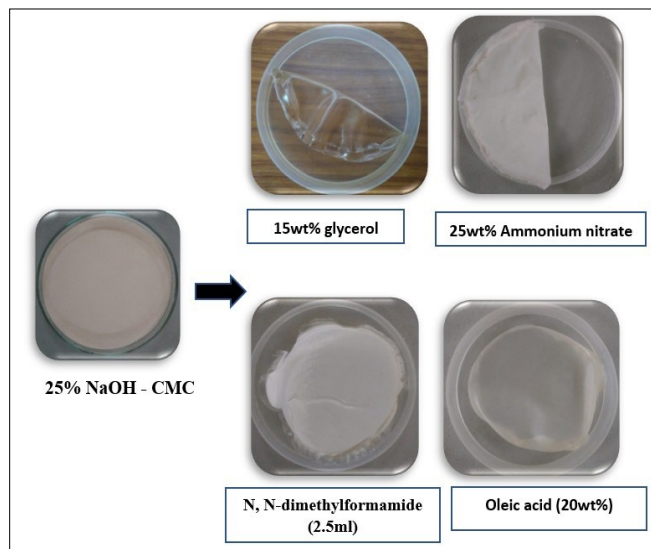


**Fig. 7.** Prepared CMC films with different concentrations with different binding agents.

### Characterization of polymer membrane electrolyte

#### Fold endurance test

The CMC films that had been created were manually put through a fold endurance test. The CMC film instantly broke apart when being folded with ammonium nitrate. It was possible to fold the CMC film with N, N-dimethylformamide, but after the second fold, it was unable to sustain the tension of folding and there were some visible cracks in the film. Even after being stretched continuously along the same fold line, the glycerol-containing CMC film was able to resist the force of folding and held together, while still maintaining a respectable degree of flexibility and increased strength. To create a cohesive, versatile and workable film, 15 wt% glycerol was added, enhancing the flexibility of the CMC film. Additionally, the CMC film with oleic acid was able to withstand breakage after folding, outperforming the glycerol film (47).

#### Colour prepared cellulose, CMC and CMC films

Table 7 shows the cellulose, CMC and CMC films' optical characteristics and surface color measured by chroma meter. The colour values of all the extracted cellulose are similar. Though the surface colour of the CMC films did not vary considerably it was affected by the type and varied concentrations during CMC film processing. As the concentration rose, CMC's b-values (blue/yellow) and ΔE-value (total colour variance) amplified, while its L-value (lightness) and a-value (green/red) diminished. The L and a-values increased the most in the CMC treated with 25% (w/v) NaOH concentration.

Furthermore, increasing the NaOH concentration up to 35% reduced the yellowness of CMC, most likely due to the initial carboxymethylation process that produces CMC (48). But, at



higher NaOH concentrations (15 and 35% w/v), all color values decreased. Therefore, the colour values of cellulose and CMC may have changed because of the carboxymethylation reaction. The CMC film with binding agent glycerol has given good L and b values when compared to other binding agents. The colour difference ( $\Delta E$ ) of CMC films varied based on the binding agent type and concentration, however, the difference was not substantial. The lowest total colour difference ( $\Delta E$ ) has been observed in the CMC film- N, N-dimethylformamide (2.5mL).

### SEM analysis of CMC films

The surface morphology demonstrates that the CMC film had a rough, uneven and black surface, indicating the presence of a semi-crystalline area in the CMC films. When different binding agents were added to the CMC powder in preparation for CMC films, the resulting films became more amorphous. This suggests an increase in the amorphous regions within the films, which increases conductivity. The amorphous area facilitates ion transport in the biopolymer electrolyte, improving conductivity by one order of magnitude. The inclusion of binding agents may improve the contact at the electrolyte-electrode interface by reducing surface roughness. Furthermore, a few cubic objects of varied sizes are seen in one location.

The smooth and brilliant morphology of the 15 wt% glycerol film surface indicates that the film became amorphous and may have helped to increase the area for rapid ionic motion, which in turn enhanced conductivity. It consists of the maximum number of pores which gives the highest conductivity. Thus, it is supported that the CMC-15 wt% Glycerol film's increased smooth and brilliant region indicates an improvement in the amorphous region. Porosity declines as a result of too much DMF. This is ascribed to the inability of the excessively non-solvent DMF to be maintained in the CMC. A few DMF droplets that had been collected were too big to create holes and the surface of the film was rough. AN (25 wt%) and OA (20 wt%) films have very few pores which results in lower conductivity. The reduced viscosity of the polymer slurry during the polymer membrane production process promotes increased porosity and the formation of larger pores (49).

### Mechanical properties and transparency of prepared CMC films

ASTM D882-80a standard method was used to measure the thickness ( $\mu\text{m}$ ), TS, EAB and YM of CMC films produced with concentrations (Table 8). The thickness of CMC films varies according to the concentration used in the film's preparation. The CMC film with oleic acid (20 wt%) has a very low thickness and its tensile properties are also weak when compared to other CMC films. The tensile characteristics (TS and EB) of the CMC films were altered depending on the CMC type and concentrations. Among the four CMC films, the best results obtained from CMC film- glycerol (15%) with the TS and EB were 2.08 MPa and 64.30% respectively, this suggested that The CMC film had a medium degree of flexibility and was strong and stiff. In CMC films, the mechanical characteristics improved linearly. The TS of CMC films was obtained after blending with four different compositions of the CMC films respectively (50).

The type of concentrations used had an impact on the CMC films' TS, EB and YM, but the effect was not statistically significant. Additionally, a hydrolysis reaction in the cellulose chain has made CMC films less flexible. Because the substituted carboxymethyl groups in an anhydrous glucopyranose unit increase the intermolecular force between the polymer chains and the ionic character, the TS value was associated with an increased DS value. However, at high NaOH concentrations, the TS value of CMC films began to decrease because of the breakdown of the polymer and the production of byproducts from sodium glycolate, which increased the CMC content reduction and lowered the intermolecular forces (51).

With a T660 of 76.40%, the CMC film containing 15% glycerol film demonstrated good transmittance against both visible and UV radiation. Next to the 15 wt% glycerol CMC film, 20 wt% oleic acid has given the transmittance of 37.76%. The transmittance for the ammonium nitrate and DMF films is relatively very low. This data suggests that CMC's size and shape could have a substantial effect on the CMC film's light absorbance (Fig. 8).

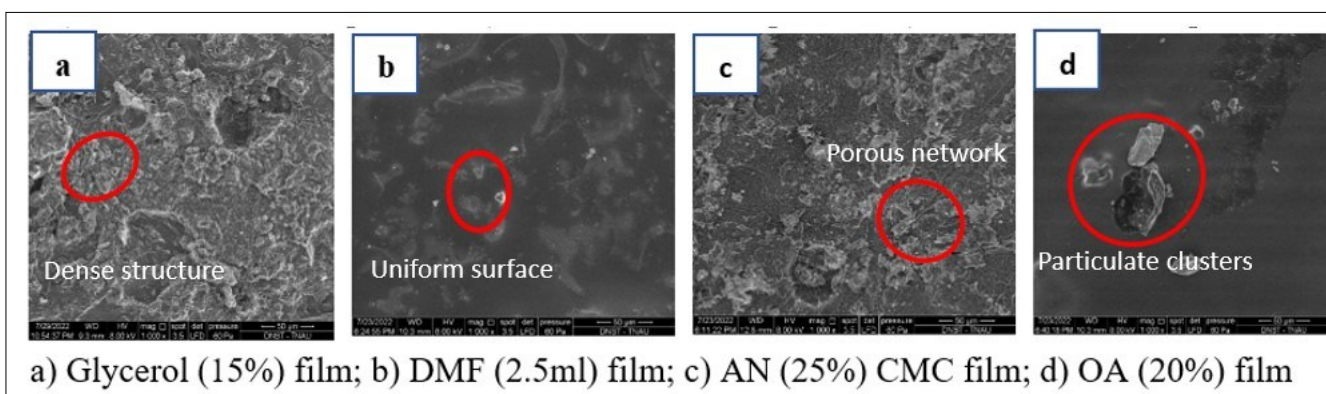


Fig. 8. SEM micrographs of CMC film.

Table 8. Mechanical characteristics and transmittance of produced CMC films at various binding agent concentrations

Film	Thickness, $\mu\text{m}$	Tensile strength, MPa	Elongation, % at Break	Young's Modulus, MPa	T <sub>660</sub> (%)
CMC film- glycerol (15 wt%)	480	2.08	64.30	1.23	76.40
CMC film-Ammonium nitrate (25 wt%)	710	7.06	22.13	3.23	8.96
CMC film- N, N-dimethylformamide (2.5mL)	400	5.51	31.44	2.52	7.21
CMC film- Oleic acid (20 wt%)	190	6.45	32.13	2.73	37.76

### Performance evaluation of prepared polymer electrolyte

The prepared polymer electrolyte was evaluated using two electrodes (Fig. 9). Aluminium sheet and copper sheet are the two electrodes. Cut these electrodes of a size of 10×3 cm each. Then the prepared polymer films were cut to the same electrode sizes. Then these electrolytes will be placed in between the two electrodes. Then the small burner should be taken and sprayed on these electrodes. After cooling, the voltage of each polymer film can be noted. Among the four polymer films, 15 wt% glycerol film has given a voltage range of 1 to 1.5 V. Next to that 20 wt% Oleic acid has given a voltage range of 0.5 to 1 V. 25 wt% Ammonium nitrate and 2.5 mL DMF do not provide stable voltage values and the voltage range was very low, nearly 0.5V (52, 53).

### Conclusion

This study highlights the potential of lignocellulosic biomass, specifically sugarcane bagasse, for the sustainable production of biodegradable polymers. Alkali pretreatment with NaOH proved effective in removing lignin and hemicellulose, enhancing cellulose recovery and decreasing crystallinity. The steam explosion technique further improved cellulose extraction, making it more suitable for conversion into CMC. XRD, FTIR and SEM analysis confirmed the structural transformation of cellulose into CMC with varying NaOH concentrations. Among the prepared CMC films, those with 15 wt% glycerol demonstrated superior flexibility, conductivity and mechanical properties, making them ideal candidates for polymer electrolyte applications. The results affirm that biomass-derived CMC can serve as a viable alternative to synthetic polymers, contributing to eco-friendly material solutions. This research paves the way for future developments in sustainable polymer production and energy storage technologies.

### Acknowledgements

We thank the financial support rendered by the scheme of ICAR-Consortia Research Platform Project (CRP) on Energy from Agriculture (EA). We also thank the Department of Renewable Energy Engineering Agricultural Engineering College and Research Institute, Tamil Nadu Agricultural University, Coimbatore for aiding in conducting the research.

### Authors' contributions

PV guided the research by formulating the concept of research and reviewing the manuscript; MRB carried out the experiment and recorded the observations; MP and PDR participated in the analysis of the data and optimizing the conditions; SP guided with the research concept, formulating research parameters and Supervision; SS involved in conceptualization, review and editing; GJ involved in analysis and writing original draft preparation; DR involved in review, editing and Supervision. All authors read and approved the final manuscript.

### Compliance with ethical standards

**Conflict of interest:** Authors do not have any conflict of interest to declare.

**Ethical issues:** None

### References

1. Duce RA, Mohnen VA, Zimmerman PR, Grosjean D, Cautreels W, Chatfield R, et al. Organic material in the global troposphere. *Rev Geophys.* 1983;21(4):921-52. <https://doi.org/10.1029/RG021i004p00921>

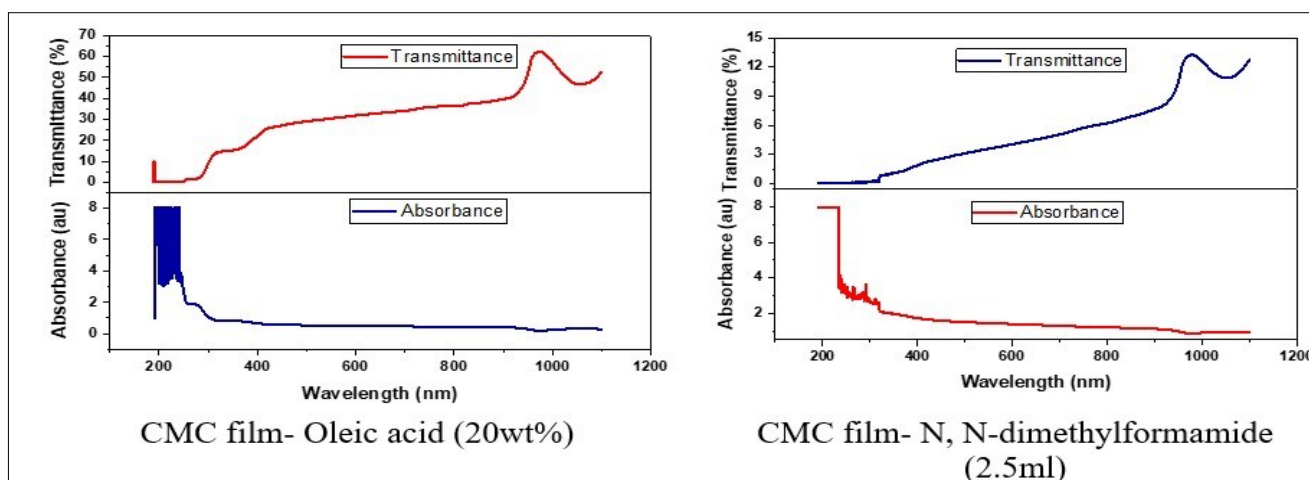


Fig. 9. UV-VIS transmittance studies of the prepared CMC film.

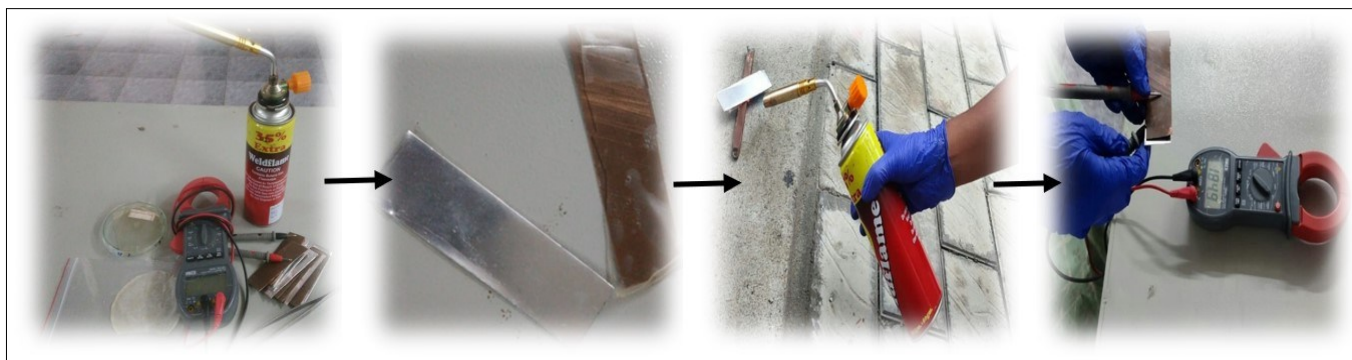


Fig. 10. Performance evaluation of prepared polymer electrolyte by cell assembly.

2. Anuar MR, Abdullah AZ. Challenges in biodiesel industry with regards to feedstock, environmental, social and sustainability issues: A critical review. *Renew Sustain Energy Rev.* 2016;58:208-23. <https://doi.org/10.1016/j.rser.2015.12.296>
3. Mori R. Replacing all petroleum-based chemical products with natural biomass-based chemical products: a tutorial review. *RSC Sustain.* 2023;1(2):179-212. <https://doi.org/10.1039/D2SU00014H>
4. Lynd LR, Beckham GT, Guss AM, Jayakody LN, Karp EM, Maranas C, et al. Toward low-cost biological and hybrid biological/catalytic conversion of cellulosic biomass to fuels. *Energy Environ Sci.* 2022;15(3):938-90. <https://doi.org/10.1039/D1EE02540F>
5. Rahman MS, Hasan MS, Nitai AS, Nam S, Karmakar AK, Ahsan MS, et al. Recent developments of carboxymethyl cellulose. *Polymers.* 2021;13(8):1345. <https://doi.org/10.3390/polym13081345>
6. Lindman B, Medronho B, Alves L, Costa C, Edlund H, Norgren M. The relevance of structural features of cellulose and its interactions to dissolution, regeneration, gelation and plasticization phenomena. *Phys Chem Chem Phys.* 2017;19(35):23704-18. <https://doi.org/10.1039/c7cp02409f>
7. Ye T, Li L, Zhang Y. Recent progress in solid electrolytes for energy storage devices. *Adv Funct Mater.* 2020;(29):2000077. <https://doi.org/10.1002/adfm.202000077>
8. Liew CW, Ramesh S. Electrical, structural, thermal and electrochemical properties of corn starch-based biopolymer electrolytes. *Carbohydr Polym.* 2015;124:222-28. <https://doi.org/10.1016/j.carbpol.2015.02.024>
9. Priya DS, Kennedy LJ, Anand GT. Effective conversion of waste banana bract into porous carbon electrode for supercapacitor energy storage applications. *Results Surf Interfaces.* 2023;10:100096. <https://doi.org/10.1016/j.rsurfi.2023.100096>
10. Zhan C, Sharma PR, He H, Sharma SK, McCauley-Pearl A, Wang R, Hsiao BS. Rice husk based nanocellulose scaffolds for highly efficient removal of heavy metal ions from contaminated water. *Environ Sci Water Res Technol.* 2020;6(11):3080-90. <https://doi.org/10.1039/D0EW00545B>
11. Yang W, Yang W, Zeng J, Chen Y, Huang Y, Liu J, Peng X. Biopolymer based gel electrolytes for electrochemical energy Storage: Advances and prospects. *Prog Mater Sci.* 2023;101264. <https://doi.org/10.1016/j.pmatsci.2024.101264>
12. Sadiq AC, Olasupo A, Ngah WSW, Rahim NY, Suah FBM. A decade development in the application of chitosan-based materials for dye adsorption: A short review. *Int J Biol Macromol.* 2021;191:1151-63. <https://doi.org/10.1016/j.ijbiomac.2021.09.179>
13. Telmo C, Lousada J, Moreira N. Proximate analysis, backwards stepwise regression between gross calorific value, ultimate and chemical analysis of wood. *Bioresour Technol.* 2010;101(11):3808-15. <https://doi.org/10.1016/j.biortech.2010.01.021>
14. Yang L, Lu M, Carl S, Mayer JA, Cushman JC, Tian E, Lin H. Biomass characterization of Agave and Opuntia as potential biofuel feedstocks. *Biomass Bioenergy.* 2015;76:43-53. <https://doi.org/10.1016/j.biombioe.2015.03.004>
15. Manisha Reddy B, Subramanian P, Sriramajayam S, Vijayakumary P, Raja K. Extraction of cellulose from banana sheath and its characterization. *Pharma Innov J.* 2022;SP-11(6):1861-67. <https://www.thepharmajournal.com/archives/2022/vol11issue6S/PartX/S-11-6-184-779.pdf>
16. Badiei M, Asim N, Jahim JM, Sopian K. Comparison of chemical pretreatment methods for cellulosic biomass. *APCBEE Procedia.* 2014;9:170-74. <https://doi.org/10.1016/j.apcbee.2014.01.030>
17. Mantovan J, Giraldo GA, Marim BM, Kishima JO, Mali S. Valorization of orange bagasse through one-step physical and chemical combined processes to obtain a cellulose-rich material. *J Sci Food Agric.* 2021;101(6):2362-70. <https://doi.org/10.1002/jsfa.10859>
18. Huang CM, Chia PX, Lim CS, Nai JQ, Ding DY, Seow PB, et al. Synthesis and characterisation of carboxymethyl cellulose from various agricultural wastes. *Cellul Chem Technol.* 2017;51(7-8):665-72. [https://www.cellulosechemtechnol.ro/pdf/CCT7-8\(2017\)/p.665-672.pdf](https://www.cellulosechemtechnol.ro/pdf/CCT7-8(2017)/p.665-672.pdf)
19. Moussa I, Khiari R, Moussa A, Belgacem MN, Mhenni MF. Preparation and characterization of carboxymethyl cellulose with a high degree of substitution from agricultural wastes. *Fibers Polym.* 2019;20:933-43. <https://doi.org/10.1007/s12221-019-8665-x>
20. Kimani PK, Kareru PG, Madivoli SE, Kairigo PK, Maina EG, Rechab OS. Comparative study of carboxymethyl cellulose synthesis from selected Kenyan biomass. *Chem Sci Int J.* 2016;17(4):1-8. <https://doi.org/10.9734/CSJI/2016/29390>
21. Khattab TA, Dacrory S, Abou-Yousef H, Kamel S. Development of microporous cellulose-based smart xerogel reversible sensor via freeze drying for naked-eye detection of ammonia gas. *Carbohydr Polym.* 2019;210:196-203. <https://doi.org/10.1016/j.carbpol.2019.01.067>
22. Roy S, Kim HJ, Rhim JW. Effect of blended colorants of anthocyanin and shikonin on carboxymethyl cellulose/agar-based smart packaging film. *Int J Biol Macromol.* 2021;183:305-15. <https://doi.org/10.1016/j.ijbiomac.2021.04.162>
23. Badry R, El-Nahass MM, Nada N, Elhaes H, Ibrahim MA. Structural and UV-blocking properties of carboxymethyl cellulose sodium/CuO nanocomposite films. *Sci Rep.* 2023;13(1):1123. <https://doi.org/10.1038/s41598-023-28032-1>
24. Mandal A, Chakrabarty D. Studies on mechanical, thermal and barrier properties of carboxymethyl cellulose film highly filled with nanocellulose. *J Thermoplast Compos Mater.* 2019;32(7):995-1014. <https://doi.org/10.1177/089270571877728>
25. Klunklin W, Jantanasakulwong K, Phimolsiripol Y, Leksawasdi N, Seesuriyachan P, Chaiyaso T, et al. Synthesis, characterization and application of carboxymethyl cellulose from asparagus stalk end. *Polymers.* 2020;13(1):81. <https://doi.org/10.3390/polym13010081>
26. Rani MS, Hassan NH, Ahmad A, Kaddami H, Mohamed NS. Investigation of biosourced carboxymethyl cellulose-ionic liquid polymer electrolytes for potential application in electrochemical devices. *Ionics.* 2016;22:1855-64. <https://www.thepharmajournal.com/archives/2022/vol11issue6S/PartX/S-11-6-184-779.pdf>
27. Tarabiah AE, Alhadlaq HA, Alaizeri ZM, Ahmed AA, Asnag GM, Ahamed M. Enhanced structural, optical, electrical properties and antibacterial activity of PEO/CMC doped ZnO nanorods for energy storage and food packaging applications. *J Polym Res.* 2022;29(5):167. <https://doi.org/10.1007/s10965-022-03011-8>
28. Demol J, Ho E, Soldenhoff K, Senanayake G. The sulfuric acid bake and leach route for processing of rare earth ores and concentrates: A review. *Hydrometallurgy.* 2019;188:123-39. <https://doi.org/10.1016/j.hydromet.2019.05.015>
29. Xu H, Li B, Mu X. Review of alkali-based pretreatment to enhance enzymatic saccharification for lignocellulosic biomass conversion. *Ind Eng Chem Res.* 2016;55(32):8691-705. <https://doi.org/10.1021/acs.iecr.6b01907>
30. Akhtar N, Gupta K, Goyal D, Goyal A. Recent advances in pretreatment technologies for efficient hydrolysis of lignocellulosic biomass. *Environ Prog Sustain Energy.* 2016;35(2):489-511. <https://doi.org/10.1002/ep.12257>
31. Aslaniyan A, Ghanbari F, Kouhsar JB, Shahraki BK. Comparing the effects of gamma ray and alkaline treatments of sodium hydroxide and calcium oxide on chemical composition, ruminal degradation kinetics and crystallinity degree of soybean straw. *Appl Radiat Isot.* 2023;191:110524. <https://doi.org/10.1016/j.apradiso.2022.110524>
32. Neenu KV, Dominic CM, Begum PS, Parameswaranpillai J, Kanoth BP, David DA, et al. Effect of oxalic acid and sulphuric acid hydrolysis on the preparation and properties of pineapple pomace derived cellulose nanofibers and nanopapers. *Int J Biol Macromol.* 2022;209:1745-59. <https://doi.org/10.1016/j.ijbiomac.2022.04.138>
33. Zhang J, Zhang W, Cai Z, Zhang J, Guan D, Ji D, Gao W. Effect of ammonia fiber expansion combined with NaOH pretreatment on the resource efficiency of herbaceous and woody lignocellulosic biomass. *ACS Omega.* 2022;7(22):18761-69. <https://doi.org/10.1021/acsomega.2c01302>

34. Hoang AT, Nizetic S, Ong HC, Chong CT, Atabani AE. Acid-based lignocellulosic biomass biorefinery for bioenergy production: Advantages, application constraints and perspectives. *J Environ Manag.* 2021;296:113194. <https://doi.org/10.1016/j.jenvman.2021.113194>
35. Loow YL, Wu TY, Md Jahim J, Mohammad AW, Teoh WH. Typical conversion of lignocellulosic biomass into reducing sugars using dilute acid hydrolysis and alkaline pretreatment. *Cellulose.* 2016;23:1491-520. <https://doi.org/10.1007/s10570-016-0936-8>
36. Duque A, Manzanares P, Ballesteros I, Ballesteros M. Steam explosion as lignocellulosic biomass pretreatment. *Biomass Fractionation Technol.* 2016;1:349-68. <https://doi.org/10.1016/B978-0-12-802323-5.00015-3>
37. Carvalheiro F, Duarte LC, Gírio F, Moniz P. Hydrothermal/liquid hot water pretreatment (autohydrolysis): A multipurpose process for biomass upgrading. *Biomass Fractionation Technol.* 2016;1:315-47. <https://doi.org/10.1016/B978-0-12-802323-5.00014-1>
38. Saurabh CK, Dungani R, Owolabi AF, Atiqah NS, Zaidon A, Aprilia NS, et al. Effect of hydrolysis treatment on cellulose nano whiskers from oil palm (*Elaeis guineensis*) fronds: Morphology, chemical, crystallinity and thermal characteristics. *BioResources.* 2016;11(3):6742-55. <https://doi.org/10.15376/biores.11.3.6742-6755>
39. Zoppe JO, Larsson PA, Cusola O. Surface modification of nano cellulosics and functionalities. *Lignocellulosics.* 2020;1:17-63. <https://doi.org/10.1016/B978-0-12-804077-5.00003-8>
40. Abraham E, Deepa B, Pothan LA, Jacob M, Thomas S, Cvelbar U, Anandjiwala R. Extraction of nanocellulose fibrils from lignocellulosic fibres: A novel approach. *Carbohydr Polym.* 2011;86(4):1468-75. <https://doi.org/10.1016/j.carbpol.2011.06.034>
41. Auxenfans T, Crônier D, Chabbert B, Paës G. Understanding the structural and chemical changes of plant biomass following steam explosion pretreatment. *Biotech Biofuels.* 2017;10:1-6. <https://doi.org/10.1186/s13068-017-0718-z>
42. Shi C, Zhang P, Chen L, Yang P, Zhao J. Effect of a thin ceramic-coating layer on thermal and electrochemical properties of polyethylene separator for lithium-ion batteries. *J Power Sources.* 2014;270:547-53. <https://doi.org/10.1016/j.jpowsour.2014.07.142>
43. Chagas R, Gericke M, Ferreira RB, Heinze T, Ferreira LM. Synthesis and characterization of dicarboxymethyl cellulose. *Cellulose.* 2020;27:1965-74. <https://doi.org/10.1007/s10570-019-02952-6>
44. Casaburi A, Rojo ÚM, Cerrutti P, Vázquez A, Foresti ML. Carboxymethyl cellulose with tailored degree of substitution obtained from bacterial cellulose. *Food Hydrocoll.* 2018;75:147-56. <https://doi.org/10.1016/j.foodhyd.2017.09.002>
45. Cherif E, Moumni H. The properties on a polysaccharide of Sodium carboxymethylcellulose (CMC) in dimethylacetamide+ acetone by conductometric study. *Phys Chem Liquids.* 2022;60(3):442-51. <https://doi.org/10.1080/00319104.2021.2012776>
46. Kamthai S, Magaraphan R. Mechanical and barrier properties of spray dried carboxymethyl cellulose (CMC) film from bleached bagasse pulp. *Indus Crops Prod.* 2017;109:753-61. <https://doi.org/10.1016/j.indcrop.2017.09.040>
47. Sadi A, Ferfera-Harrar H. Cross-linked CMC/gelatin bio-nanocomposite films with organoclay, red cabbage anthocyanins and pistacia leaves extract as active intelligent food packaging: colorimetric pH indication, antimicrobial/antioxidant properties and shrimp spoilage tests. *Int J Biol Macromol.* 2023;242:124964. <https://doi.org/10.1016/j.ijbiomac.2023.124964>
48. Basu P, Narendrakumar U, Arunachalam R, Devi S, Manjubala I. Characterization and evaluation of carboxymethyl cellulose-based films for healing of full-thickness wounds in normal and diabetic rats. *ACS Omega.* 2018;3(10):12622-32. <https://doi.org/10.1021/acsomega.8b02015>
49. Shui T, Feng S, Chen G, Li A, Yuan Z, Shui H, et al. Synthesis of sodium carboxymethyl cellulose using bleached crude cellulose fractionated from cornstalk. *Biomass Bioenergy.* 2017;105:51-58. <https://doi.org/10.1016/j.biombioe.2017.06.016>
50. Esteghlal S, Niakousari M, Hosseini SM. Physical and mechanical properties of gelatin-CMC composite films under the influence of electrostatic interactions. *Int J Biol Macromol.* 2018;114:1-9. <https://doi.org/10.1016/j.ijbiomac.2018.03.079>
51. Rachtanapun P, Thanakkasaranee S, Auras RA, Chaiwong N, Jantanasakulwong K, Jantrawut P, et al. Morphology, mechanical and water barrier properties of carboxymethyl rice starch films: sodium hydroxide effect. *Molecules.* 2022;27(2):331. <https://doi.org/10.3390/molecules27020331>
52. Wang F, Wu X, Yuan X, Liu Z, Zhang Y, Fu L, et al. Latest advances in supercapacitors: from new electrode materials to novel device designs. *Chem Soc Rev.* 2017;46(22):6816-54. <https://doi.org/10.1039/C7CS00205J>
53. Xie P, Yuan W, Liu X, Peng Y, Yin Y, Li Y, Wu Z. Advanced carbon nanomaterials for state-of-the-art flexible supercapacitors. *Energy Stor Mater.* 2021;36:56-76. <https://doi.org/10.1016/j.ensm.2020.12.011>